Double-Stranded DNA Single-Walled Carbon Nanotube Hybrids for Optical Hydrogen Peroxide and Glucose Sensing

Yang Xu,[†] Pehr E. Pehrsson,[‡] Liwei Chen,[§] Ru Zhang,[§] and Wei Zhao*[,†]

Department of Chemistry, University of Arkansas, 2801 South University Avenue, Little Rock, Arkansas 72204, Chemistry Division, Naval Research Laboratory, Washington, DC 20375, and Department of Chemistry and Biochemistry, Ohio University, Athens, Ohio 45701

Received: February 3, 2007; In Final Form: April 5, 2007

The unique optical properties of semiconducting single-walled carbon nanotubes (SWNTs) are exquisitely sensitive to variations in the surrounding environments. Here, we have studied the redox chemistry of SWNTs encased with double-stranded deoxyribonucleic acid (DNA) reacted with either hydrogen peroxide H_2O_2 or glucose in the presence of the glucose oxidase enzyme. The DNA-SWNT hybrids are prepared in aqueous solution by sonication that cuts the DNA into short fragments of 100−300 base pairs which efficiently wrap individual nanotubes. The DNA-SWNT hybrids are optically sensitive to H_2O_2 and glucose, and the hybrid surface can be regenerated by dialytically removing the hydrogen peroxide. This study reinforces the potential of DNA-SWNT hybrids for use in immunoassays and glucose sensing.

Introduction

Single-walled carbon nanotubes (SWNTs) can be viewed as the one-dimensional form of fullerenes.[1] SWNTs can easily align themselves by van der Waals force between tubes to form ropes or bundles that are typically 10−25 nm in diameter and a few micrometers long.[1] This behavior makes them difficult to disperse in solution. Different covalent[2−6] and noncovalent[7−17] surface functionalization approaches have been used to change the SWNT surface to make them water soluble and suitable for biological and medical research. For example, with sonication, double-stranded deoxyribonucleic acids (dsDNAs) solubilize individual SWNTs to form stable suspensions in aqueous solution.[16,17] In comparison with single-stranded deoxyribonucleic acids (ssDNAs) which are highly efficient to disperse SWNTs in water,[11,12] dsDNAs are less costly and easier to obtain from natural sources. Therefore, in this paper, we focus on the dsDNA-SWNT hybrids.

There is intense interest in using DNA-SWNT hybrids as a biosensor component for optical sensing.[16,18] The unique structural properties of SWNT, particularly their large surface area to weight ratio, make them extremely useful as a carrier for macromolecular enzymes and DNA. One of the key issues in the enzyme-immobilized biosensor design is the establishment of a fast electron transfer between the enzyme active site and the target component.[19] H_2O_2, as one of the main products for many enzyme-catalyzed reactions, has been found to react with HiPco carbon nanotubes which are wrapped with sodium dodecyl sulfate (SDS) in aqueous solution.[20] On the other hand, the mechanism of the reaction on dsDNA-encased SWNTs is unclear. In our previous work, we have studied preliminarily their pH-dependent near-infrared optical properties.[16] However, the structure of the dsDNA-SWNT hybrids and their redox behaviors were not systematically examined in this system. In this work, we first studied the structural changes of dsDNA and their SWNT hybrids under the impact of sonication and then investigated the redox reactions of the hybrids with H_2O_2 and glucose in the presence of glucose oxidase (GOx) enzyme by monitoring the near-infrared optical changes of the semiconducting nanotubes. In addition, the reversibility of the near-infrared spectral intensity of H_2O_2-reacting semiconducting nanotubes was examined by tuning pH and by using dialysis to remove H_2O_2 molecules, which regenerates and reactivates the dsDNA-SWNT surfaces. This investigation may provide us with a useful approach for biomedical sensing applications such as diabetes diagnostics.

Experimental Section

Materials. Raw HiPco SWNTs (lot no. 79, December 2, 2001) were purchased from Carbon Nanotechnologies, Inc. with sizes ranging from 0.7 to 1.1 nm in diameter and a few hundred nanometers long.[20] Double-stranded deoxyribonucleic acid (dsDNA) from salmon testes, glucose oxidase (EC 1.1.3.4, 196 units/mg) from *Aspergillus niger*, α-D-glucose (>99% pure), β-D-glucose (>97%), H_2O_2 (30 wt %), and sodium dodecyl sulfate (SDS) (>99% GC) were obtained from Sigma-Aldrich. Agarose low EEO gel (electrophoresis grade) was purchased from Fisher Scientific. The 250−10 000 bp DNA marker and the 8∼587 bp pBR322 DNA/*Bsu*RI (H*ae*III) ladder were from Fermentas Life Science.

Sample Preparation. The dispersion procedure for DNA-SWNT suspensions was as follows:[16] 0.4 mg of SWNTs was added to 5 mL of dsDNA (0.7 mg/mL) TE buffer solution (10 mM, pH = 7.3) and then was sonicated in an ice−water bath (Branson Model 1510R-MT, 42 kHz, output power 70 W) for 1 h followed by centrifugation (Galaxy 16 microcentrifuge, VWR International) for 15 h at 16 000*g* to remove undispersed SWNTs.[20]

* To whom correspondence should be addressed. Phone: (501) 569-8823. E-mail: wxzhao@ualr.edu.
[†] University of Arkansas at Little Rock.
[‡] Naval Research Laboratory.
[§] Ohio University.

10.1021/jp0709611 CCC: $37.00
Published on Web 05/27/2007

Reaction Procedures. For the H_2O_2 reaction, a H_2O_2 solution (0.6 wt %) in different volumes was added to 0.3 mL samples of DNA-HiPco suspension in 1 mm path length quartz cells to make H_2O_2 concentrations from 0 to 200 ppm.

To dialytically remove H_2O_2, the H_2O_2-reacted dsDNA-HiPco nanotube sample was placed into a dialysis membrane (6000−8000 MWCO, Spectrum Laboratories Inc.) which was kept in pH 7.3 TE buffer. The buffer solution was stirred constantly during dialysis and was replaced by fresh solution every hour. The nanotube sample was removed from the membrane periodically for spectral measurements.

Spectral reversibility under pH tuning was tested by pH titration with 0.5 M NaOH or 0.5 M HCl solutions. The pH was measured using an Orion Model 420 pH meter with a Thermo Electron Orion micro pH glass electrode. The spectrum of the suspension was measured 2 min after each pH adjustment.

For glucose-related experiments, fresh glucose oxidase solution was prepared by dissolving 10 mg of GOx in 5 mL of TE buffer solution. Twenty units of GOx were mixed with the dsDNA HiPco solution to get a GOx-dsDNA-SWNT mixture. For the glucose solution, 0.1 g each of α-D-glucose and β-D-glucose powders was dissolved into 0.5 mL of distilled water. Immediately after the sample was dissolved, 2 μL of the solution was injected into 0.45 mL of the GOx-DNA-HiPco nanotube sample to make a 5 mM glucose mixture.

All samples were measured in 1 mm path length quartz cells using a UV−vis-NIR absorption spectrometer (Lambda 19, Perkin-Elmer) at room temperature to record the time-dependent absorption spectra. To correct for the effects of dilution on the spectral intensity (the absorbance), all spectra in this work are normalized to the band at 988 nm which is insensitive to H_2O_2 and pH changes.

Sample Characterization. For DNA length determination, gel electrophoresis analysis was conducted for dsDNA and dsDNA wrapped nanotubes. A 2% w/v agarose gel was prepared by heating agarose powder mixed with electrophoresis buffer Tris-acetate-EDTA (TAE) in a microwave oven until all the agarose powder had melted. This mixture was cooled to 50−60 °C and then was cast onto a gel tray set (10.7 × 6 cm) with a 12-tooth comb, around which the molten agarose (gel) was formed. Then, the gel tray was inserted horizontally into a minigel electrophoresis chamber (Labnet International Inc., NJ) and was barely covered with TAE buffer working solution. Twelve microliters of each sample was loaded into the individual wells, and an electrophoresis power supply Gel XL PlusTM was set to 100 V. When the markers had moved three-fourths of the way up the gel, it turned off automatically. The gel tray was removed from the tank and was placed in a dish containing ethidium bromide, a fluorescent dye used for staining nucleic acid. The gel was stained for 15−20 min and then was visualized under a UV transilluminator (Spectroline TE-312S longlife filter Highest Ultraviolet, Spectronics Co.).

For atomic force microscope (AFM) imaging, a few drops of 1 M $MgCl_2$ solution were applied to a freshly cleaved mica substrate; the substrate was then rinsed with distilled water, and dsDNA-SWNT sample solutions were applied for 1 min and then were blown dry with argon gas. Images were captured under ambient conditions in AC mode using an Asylum Research MFP3D microscope (Santa Barbara, CA). AFM probes with 60−80 kHz resonant frequencies were used, and the resulting images were processed with the Igor Pro (WaveMetrics, Inc., Portland, OR) software package.

Raman spectra measurements were made using a Renishaw MicroRaman 1000 Spectrometer with 514 nm Ar^+ laser and 785 nm diode laser excitation sources. The spectra were calibrated with Si standards.

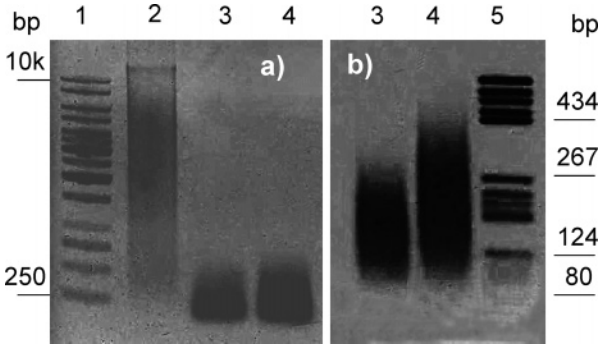

Figure 1. Gel electrophoresis analysis of dsDNA using two different markers 250−10 000 bp DNA marker (a) and the 8∼587 bp pBR322 DNA/*Bsu*RI (H*ae*III) ladder (b). The use of the shorter marker in b allows one to see the details of shortened samples. (1) 250−10k bp marker, (2) unsonicated dsDNA, (3) sonicated dsDNA, (4) sonicated dsDNA-SWNT, and (5) 8−587 bp marker.

Results and Discussion

Structure of dsDNA-SWNT Hybrids. Figure 1 shows the gel electrophoresis analysis of a dsDNA solution and a dsDNA wrapped HiPco nanotube suspension, both of which were prepared with 1 h sonication. A dsDNA sample without sonication was also analyzed for comparison, and it shows a broad base pair (bp) distribution of ∼300−10 000. However, after 1 h of sonication, the dsDNAs are shortened to ∼100−300 base pairs. Owing to the cavitation and direct mechanical or thermal degradation mechanisms, ultrasonication of the aqueous DNA solution cuts the DNA helix into fragments.[21] Our result is consistent with ref 21 where the molecular weight of the DNA fragments decreases under sonication and approaches a lower limit of 100−500 base pairs. For the dsDNAs encased HiPco SWNT sample, short dsDNA lengths of ∼100−300 base pairs are observed under the same ultrasonication condition. As shown in Figure 1b, the band is elongated as compared to the dsDNA alone, suggesting that the DNA might come with the wrapped nanotubes in the electrophoresis.

This observation is corroborated by topographic imaging of the dsDNA-SWNT complexes using AFM. The image in Figure 2 shows that SWNTs are individually dispersed in the dsDNA solution. The profiles of the SWNTs in this figure show that the height of the complexes varies from 0.8 nm to 1.8 nm. There are parts of a tube about 0.2 nm or 0.4 nm higher than other parts of the same tube. Since the height of dsDNA in our imaging condition is 0.2−0.4 nm (obtained from other images not shown in Figure 2 from the same sample, which is in agreement with literature),[22,23] this suggests that the SWNTs are dispersed in the aqueous environment because of dsDNA coating, and the coating may have different thicknesses.

Reaction with H_2O_2. The near-infrared (NIR) spectra of dsDNA-SWNT suspensions were red-shifted by 20−30 nm (Figure 1S, Supporting Information) as compared to that of SDS-wrapped SWNTs,[8,20,24] probably because the introduction of new wrapping molecules altered the electronic dispersion. The absorption features from 1100 to 1350 nm correspond to the first interband transition S_{11} bands of semiconducting nanotubes,[8,24−27] each of which could be assigned to a nanotube of specific diameter and chirality. The most sensitive S_{11} bands in DNA solution at 1275, 1195, and 1130 nm correspond to (10, 5), (12, 1), and (9, 4), with diameters of 1.050, 0.995, and 0.916 nm, respectively. In our previous work,[20] we found that these

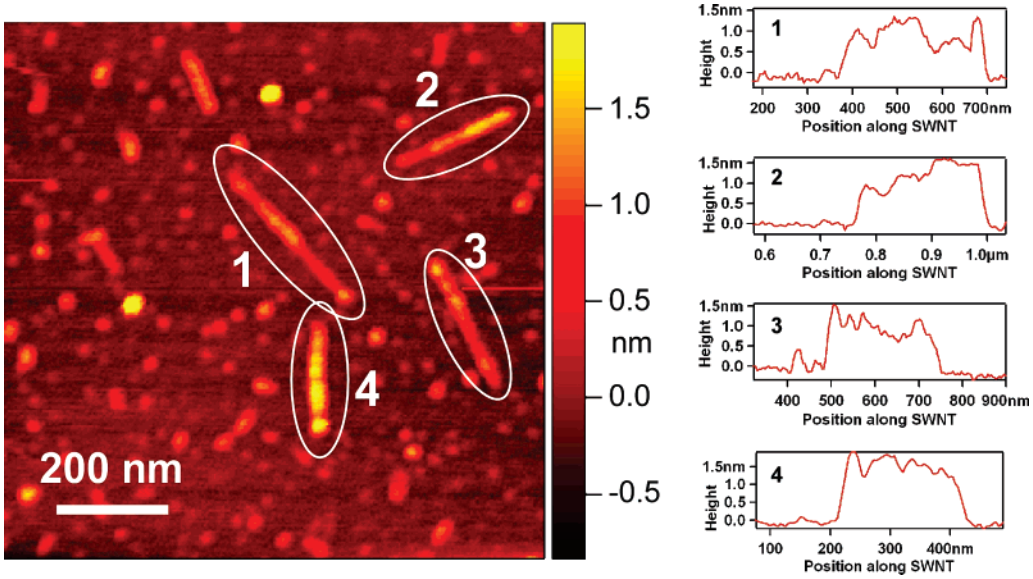

Figure 2. An AFM image of dsDNA-wrapped HiPco SWNTs on mica. The height profiles of four tubes are shown to the right.

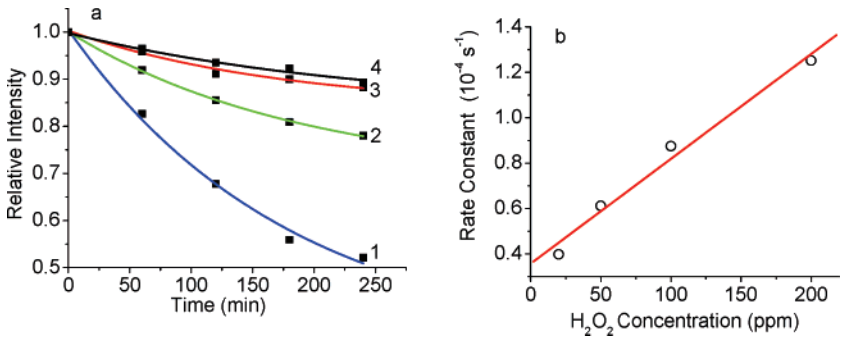

Figure 3. (a) The intensity of the S_{11} band at 1278 nm (plotted as the ratio S_{1278nm}/S_{988nm}) with reaction time for dsDNA-SWNT suspensions after addition of H_2O_2 at different concentrations. 1: 200 ppm, 2: 100 ppm, 3: 50 ppm, and 4: 20 ppm. The solid lines are exponential fits. (b) Rate constants obtained from a are plotted as a function of H_2O_2 concentration.

NIR bands of SDS encased nanotubes are very sensitive to oxidation by hydrogen peroxide. For dsDNA-SWNT samples, the 1275 nm band of larger diameter nanotubes ((10, 5), d = 1.050 nm) with a smaller band gap is more sensitive to the H_2O_2. The band intensity decreases dramatically and it almost disappears after reacting with 200 ppm of H_2O_2 for 4 h. The (10, 5) nanotubes have a more negative potential (about −0.60 V vs normal hydrogen electrode NHE) than the smaller nanotubes (9, 4) with d = 0.916 nm (−0.25 V vs NHE),[28] so the (10, 5) nanotubes are a stronger reductant and more likely transfer electrons to the oxidant H_2O_2 molecules, which have a relative high reduction potential (E_0 = 1.77 V, and E = 1.26 at pH 7.3).[20]

Figure 3a shows the time-dependent intensity change of the 1275 nm band of a dsDNA-HiPco nanotube suspension after adding different concentrations of H_2O_2. Semiconducting SWNTs are more reactive than metallic SWNTs because hole-doping by H_2O_2 results in faster oxidation. Only the first van Hove transition diminishes, while the second semiconductor van Hove transition shows little change. As the H_2O_2 concentration increases from 20 to 200 ppm, the relative intensity decreases more rapidly and follows a different exponential decay rate. There is a linear relationship between the rate constant and the H_2O_2 concentration as shown in Figure 3b, suggesting that the reaction follows a pseudo-first-order kinetic behavior, which is similar to the result of Doorn and his co-workers who found a linear change in rate constant with change in organic acceptor concentration.[28]

Regeneration is one of the most important requirements for sensor applications, so several cycling experiments were run to demonstrate this capability. For example, a dsDNA-HiPco nanotube sample was reacted with 100 ppm of hydrogen peroxide for 4 h, which reduced the relative absorbance of the S_{11} band from 1 to about 0.70. When the mixture was dialyzed, the spectral properties of the carbon nanotubes gradually recovered, as shown in Figure 4a. The concentration differential induced by dialysis removed the hydrogen peroxide and gradually returned the nanotubes to their original state. Since their surface activity recovered, we infer that hydrogen peroxide formed an electron-localizing complex such as endoperoxide on the nanotube surfaces. Brus surmised that oxygen played a similar role in SWNT aqueous suspensions, in which surface oxygen complexes with a nanotube and, upon protonation, injects a hole into its π-electron valence band.[29] H_2O_2 molecules may play a similar role. Dialysis released the H_2O_2 from the carbon nanotube surfaces, suggesting that the formation of the complex is reversible. Figure 4b shows that the reaction dialysis cycle returns the nanotube sample to its initial state and that it can be recycled several times without losing reactivity with H_2O_2.

The recoverability of H_2O_2-reacted dsDNA-SWNT samples was also demonstrated by changing the sample pH. Figure 5a shows the recovery of the SWNT spectral features as the pH is increased from 7.3 to 11. This phenomenon might be related to two possible mechanisms discussed in our previous work.[16] One is that pH induces partial base pair separation or combination

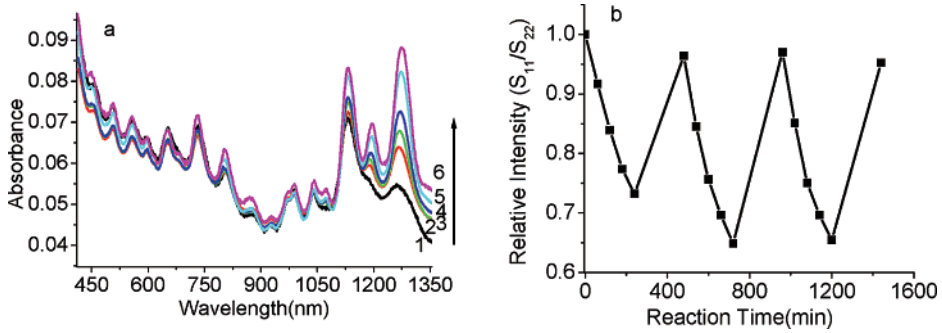

Figure 4. (a) Dialytic recovery of the spectral intensity of a dsDNA-SWNT suspension reacted with 100 ppm H_2O_2: (1) reaction with H_2O_2 overnight, (2−6) dialysis for 1, 2, 3, 4, and 16 h; (b) reproducibility curve of an SWNT sample after reaction with 100 ppm H_2O_2 and then dialysis to recover the spectral intensity (As_{1278nm}/As_{988nm}) for three repeating cycles.

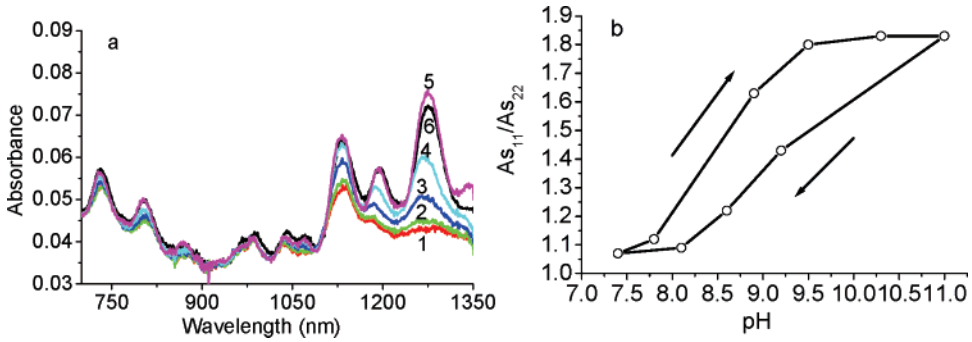

Figure 5. (a) Absorption spectra from a dsDNA-SWNT suspension reacted with 200 ppm H_2O_2 at various pHs: (1) 7.4, (2) 8.1, (3) 8.6, (4) 9.2, (5) 11.0, and (6) before addition of H_2O_2 at pH 7.4; (b) pH-induced changes in the absorbance ratio (As_{1278nm}/As_{988nm}) of a sample containing 200 ppm H_2O_2.

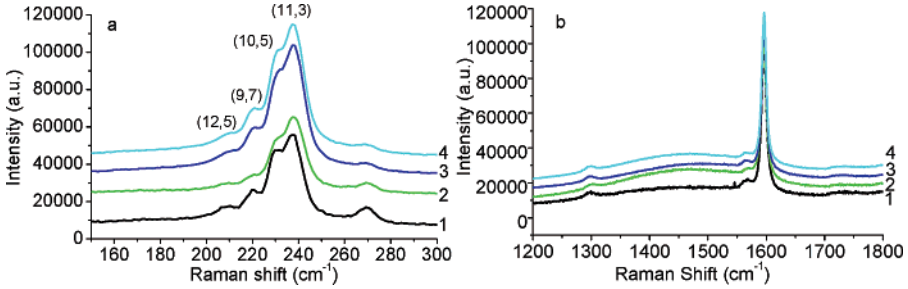

Figure 6. Raman spectra (785 nm excitation) of dsDNA-SWNT suspensions: (1) pH 7.3; (2) after addition of 200 ppm H_2O_2 sample 1; (3) after increasing the pH of sample 2 to 11; and (4) after dialytic removal of H_2O_2 from sample 2.

in the double-stranded DNA which changes the SWNT valence electron density and restores or weakens the interband transition.[30] The other is that pH changes the H_2O_2 reduction potential.[20] In addition, H_2O_2 converts to HO_2^- in basic solutions and is repelled from the negatively charged surface of dsDNA-nanotubes, which hinders electron transfer in the redox reaction.[20] Other work examined the pH dependent reaction of O_2 dissolved in aqueous solution with SWNTs, and the reactivity is completely reversible as the solution pH is cycled from acidic to basic conditions.[2,29,31] Addition of NaOH increases the solution pH to 11 and totally restores the NIR intensities. On the other hand, when HCl is added into the recovered solution, the NIR features are almost obliterated. As shown in Figure 5b, the recovery process of the S_{11} peak relative intensity exhibits hysteresis. The hysteresis in part reflects the time needed for reaching a pH equilibrium on SWNT surface. When the original pH is restored, the charge distribution change on SWNT surface may lag behind, which is a time-dependent process, as reflected in the UV−vis−NIR absorption spectra. The detailed study will be reported elsewhere.

Resonant Raman spectroscopy was used to characterize the reaction of H_2O_2 with SWNTs. The Raman tangential mode (G band) at ~1600 cm^{-1} arises from the C−C vibrations in sp^2 hybridized systems, which split into high- and low-frequency phonons. The broad peak (D band) at around 1300 cm^{-1} is related to disorder and defects in the graphitic structure of the nanotubes. The radial breathing modes (RBM) are around 200−300 cm^{-1}. The RBM frequency depends inversely on the tube diameter.[32,33] Figure 6 shows Raman spectra taken with a 785 nm (1.58 eV) excitation laser, where only semiconducting nanotubes are excited because of resonant excitation into the second valence to conduction band transitions (S_{22}) of semiconducting nanotubes.

Reaction of semiconducting SWNTs with hydrogen peroxide suppresses the radial breathing modes from 200 cm^{-1} to 250 cm^{-1} because of electron density loss[20] from the nanotubes with different diameters, including the (10, 5), (9, 7), and (12, 5) tubes. The Raman intensity almost recovers after removal of the H_2O_2 through dialysis of the dsDNA-SWNT suspension, presumably because dialysis removes the hydrogen peroxide from the charge-transfer complex on the nanotube surfaces. Likewise, increasing the solution pH restores the Raman intensity since the electronic structure of the SWNTs recovers in the basic solution. It is noticed that addition of H_2O_2 might

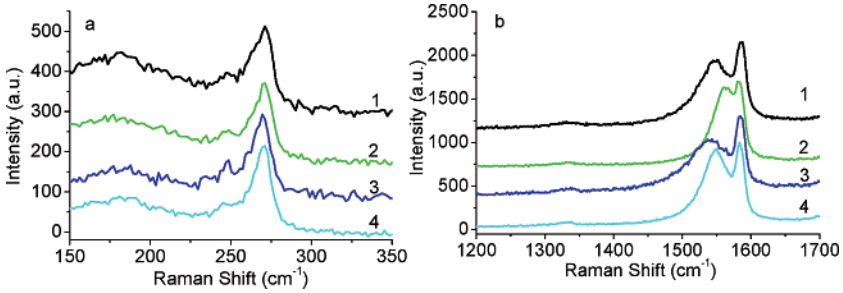

Figure 7. Raman spectra (514 nm excitation) of dsDNA-SWNT suspensions: (1) pH 7.3; (2) after addition of 200 ppm H_2O_2 to sample 1; (3) after increasing the pH of sample 2 to 11; and (4) after dialytic removal of H_2O_2 from sample 2.

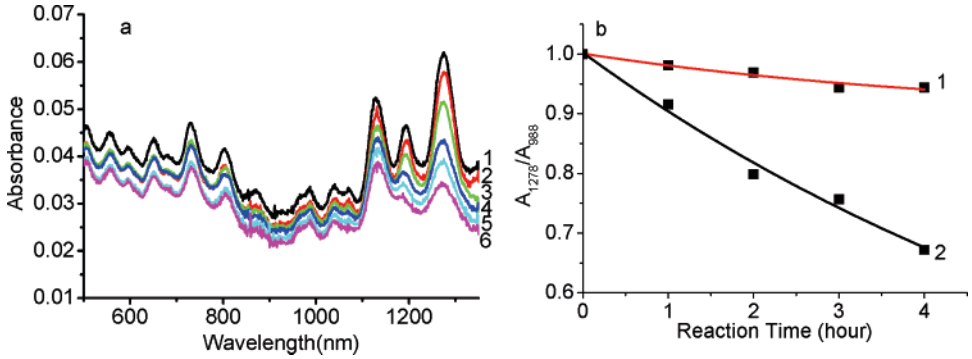

Figure 8. (a) Changes of absorption spectra of a dsDNA-SWNT suspension in TE buffer before (1) and after (2) addition of 20 units GOx; (3−6) 1, 2, 3, and 4 h after addition of 5 mM β-D-glucose, respectively; (b) relative intensity A_{1278nm}/A_{988nm} changes as a function of reaction time for α-D-glucose (1) and β-D-glucose (2).

not cause bundle formation in the dsDNA-SWNT sample as occurred in the SDS-SWNT sample,[20] as indicated by the lack of (10, 2) nanotube enhancement at 270 cm^{-1}.[28] Therefore, DNA-encased nanotubes could be more stable to external environmental perturbations than those encased with SDS.

Figure 7 shows the Raman spectra under the excitation of a 514 nm (2.41 eV) laser which primarily excites metallic nanotubes. The RBM Raman spectra of the metallic nanotubes were largely unchanged by addition of H_2O_2, reflecting a minimal change in their electronic density of states. However, addition of H_2O_2 changed the shape of their Breit−Wigner−Fano (BWF) feature around the G mode by weakening its intensity. Removal of the H_2O_2 or increasing the suspension pH restores the BWF feature.

One must consider the possibility that the observed spectral changes are related to SWNT aggregation rather than to electronic changes induced by the redox reaction between SWNTs and H_2O_2. Raman spectroscopy is sensitive to aggregation,[34] and on the basis of our spectra, there is little evidence of changes in aggregation during the various chemical treatments. However, a recent paper[12] concluded that optical absorption spectroscopy and Raman scattering are less sensitive to aggregation than NIR fluorescence or small-angle neutron scattering (SANS). In future experiments, we will use SANS to confirm that aggregation does not significantly affect our results.

Reaction with Glucose Catalyzed by Glucose Oxidase. Hydrogen peroxide is the main product of the GOx-catalyzed glucose reaction,[35] so the spectral sensitivity of dsDNA-SWNT to the glucose was tested with this reaction. Glucose has α- and β-anomers which are in equilibrium (36:64 in molar ratio) in aqueous solution at room temperature.[36] Glucose oxidase is specific for the β-anomers of D-glucose, which catalyzes the oxidation of β-D-glucose to D-glucono-1, 5-lactone, and hydrogen peroxide using molecular oxygen as the electron acceptor. Therefore, it is expected that β-anomers should alter the spectra of SWNTs more rapidly than α-anomers, because the latter must first mutarotate into β-anomers before reaction. The general range of blood glucose concentration in healthy and diabetic persons is about 3−8 mM and 9−40 mM, respectively.[35,37] Here, 5 mM β-D-glucose was added into the dsDNA-SWNT samples in the presence of 20 units of GOx. The H_2O_2 product reacted with the SWNTs and depleted their valence electrons, so the NIR absorption bands from 1000∼1300 nm weakened with reaction time. This suppression rate increases with the nanotube diameter, as shown in Figure 8a, just as with the H_2O_2 reaction. In addition, Figure 8b shows that the two different glucose anomers have different reactivities as monitored by the spectral change of the SWNTs. After 4 h, the spectral intensity change of β-D-glucose was about 7 times larger than that of the α-anomers. The result confirmed glucose oxidase's reaction specificity for β-anomers and suggests that dsDNA-SWNTs may be used to monitor the mutarotation process of glucose anomers.

Conclusions

In this work, we first examined how dsDNA wrapping with sonication affects SWNT dispersion in aqueous solution and observed that shortened dsDNA is more efficient at covering individual SWNTs than pristine DNA strands. We examined the redox chemistry of dsDNA-treated SWNTs under pH conditions mimicking those in the human body, using hydrogen peroxide and the α- and β-glucose anomers in the presence of the GOx enzyme. For the H_2O_2 reaction, the reaction follows pseudo-first-order kinetics. Regeneration is achieved by dialytically removing the H_2O_2 or increasing the pH. The redox reaction is more efficient for β-anomers than α-anomers which need to first mutarotate into β-anomers before reaction. The results suggest that dsDNA-encased SWNTs may be useful in hydrogen peroxide and glucose biosensors for chemical, biological, clinical, and medical applications.[35]

Acknowledgment. We thank Dr. Qingfang He for his assistance in the gel electrophoresis analysis. This work was supported by ARO under Award No. DAAD 190210140, ONR, and Defense Threat Reduction Agency.

Supporting Information Available: The effect of dsDNA length on the SWNT dispersion. This material is available free of charge via the Internet at http://pubs.acs.org.

References and Notes

(1) Dresselhaus, M. S.; Dresselhaus, G.; Eklund, P. C. *Science of Fullerenes and Carbon Nanotubes*; Academic Press: New York, 1996.

(2) Zhao, W.; Song, C.; Pehrsson, P. E. *J. Am. Chem. Soc.* **2002**, *124*, 12418−12419.

(3) Coleman, K. S.; Bailey, S. R.; Fogden, S.; Green, M. L. H. *J. Am. Chem. Soc.* **2003**, *125*, 8722−8723.

(4) Georgakilas, V.; Kordatos, K.; Prato, M.; Guldi, D. M.; Holzinger, M.; Hirsch. A. *J. Am. Chem. Soc.* **2002**, *124*, 760−761.

(5) Dyke, C. A.; Tour, J. M. *J. Am. Chem. Soc.* **2003**, *125*, 1156−1157.

(6) Hill, D. E.; Lin, Y.; Rao, A. M.; Allard, L. F.; Sun, Y.-P. *Macromolecules* **2002**, *35*, 9466−9471.

(7) O'Connell, M. J.; Boul, P.; Ericson, L. M.; Huffman, C.; Wang, Y.; Haroz, E.; Kuper, C.; Tour, J.; Ausman, K. D.; Smalley, R. E. *Chem. Phys. Lett.* **2001**, *342*, 265−271.

(8) O'Connell, M. J.; Bachilo, S. M.; Huffman, C. B.; Moore, V. C.; Strano, M. S.; Haroz, E. H.; Rialon, K. L.; Boul, P. J.; Noon, W. H.; Kittrell, C.; Ma, J.; Hauge, R. H.; Weisman, R. B.; Smalley, R. E. *Science* **2002**, *297*, 593−596.

(9) Chen, R. J.; Zhang, Y.; Wang, D.; Dai, H. *J. Am. Chem. Soc.* **2001**, *123*, 3838−3839.

(10) Star, A.; Liu, Y.; Grant, K.; Ridvan, L.; Stoddart, J. F.; Steuerman, D. W.; Diehl, M. R.; Boukai, A.; Heath, J. R. *Macromolecules* **2003**, *36*, 553−560.

(11) Zheng, M.; Jagota, A.; Semke, e. D.; Diner, B. A.; Melean, R. S.; Lustig, S. R.; Richardson, R. E.; Tassi, N. G. *Nat. Mater.* **2003**, *2*, 338−342.

(12) Fagan, J. A.; Landi, B. J.; Mandelbaum, I.; Simpson, J. R.; Bajpai, V.; Bauer, B. J.; Migler, K.; Hight Walker, A. R.; Raffaelle, R.; Hobbie, E. K. *J. Phys. Chem. B* **2006**, *110*, 23801−23805.

(13) Wang, H.; Hobbie, E. K. *Langmuir* **2003**, *19*, 3091−3093.

(14) Wang, H.; Zhou, W.; Ho, D. L.; Winey, K. L.; Fischer, J. E.; Glinka, C. J.; Hobbie, E. K. *Nano Lett.* **2004**, *4*, 1789−1793.

(15) Zhao, J.; Lu, Jian, P.; Han, J.; Yang, C. K. *Appl. Phys. Lett.* **2003**, *82*, 3746−3748.

(16) Kelley, K.; Pehrsson, P. E.; Ericson, L. M.; Zhao, W. *J. Nanosci. Nanotechnol.* **2005**, *5*, 1041−1044.

(17) Nakashima, N.; Okuzono, S.; Murakami, H.; Nakai, T.; Yoshikawa, K. *Chem. Lett.* **2003**, *32*, 456−457.

(18) Zheng, M.; Diner, B. A. *J. Am. Chem. Soc.* **2004**, *126*, 15490−15494.

(19) Sotiropoulou, S.; Chaniotakis, N. A. *Anal. Bioanal. Chem*. **2003**, *375*, 103−105.

(20) Song, C.; Pehrsson, P. E.; Zhao, W. *J. Phys. Chem. B* **2005**, *109*, 21634−21639.

(21) Elsner, H. I.; Lindblad, E. B. *DNA-J. Mol. Cell. Biol*. **1989**, *8*, 697−701.

(22) Uchihashi, T.; Tanigawa, M.; Ashino, M.; Sugawara, Y.; Yokoyama, K.; Morita, S.; Ishikawa, M. *Langmuir* **2000**, *16*, 1349−1353.

(23) Chen, L.; Yu, X.; Wang, D. *Ultramicroscopy* **2007**, *107*, 275−280.

(24) Benedict, B.; Pehrsson, P. E.; Zhao, W. *J. Phys. Chem. B* **2005**, *109*, 7778−7780.

(25) Saito, R.; Dresselhaus, G.; Dresselhaus, M. S. *Physical properties of carbon nanotubes;* Imperial College Press: London, 1998.

(26) Chou, S. G.; Ribeiro, H. B.; Barros, E. B.; Santos, A. P.; Nezich, D.; Samsonidze, G. G.; Fantini, C.; Pimenta, M. A.; Jorio, A.; Filho, F. P.; Dresselhaus, M. S.; Dresselhaus, G.; Saito, R.; Zheng, M.; Onoa, G. B.; Semke, E. D.; Swan, A. K.; Unlu, M. S.; Goldberg, B. B. *Chem. Phys. Lett*. **2004**, *397*, 296−301.

(27) Weisman, R. B.; Bachilo, S. M. *Nano Lett.* **2003**, *3*, 1235−1238.

(28) O'Connell, M. J.; Eibergen, E. E.; Doorn, S. K. *Nat. Mater*. **2005**, *4*, 412−418.

(29) Dukovic, G.; White, B. E.; Zhou, Z.; Wang, F.; Jockusch, S.; Steigerwald, M. L.; Heinz, T. F.; Friesner, R. A.; Turro, N. J.; Brus, L. E. *J. Am. Chem. Soc.* **2004**, *126*, 15269−15276.

(30) Itkis, M. E.; Niyoge, S.; Meng, M. E.; Hamon, M. A.; Hu, H.; Haddon, R. C. *Nano Lett.* **2002**, *2*, 155−159.

(31) Strano, M. S.; Huffman, C. B.; Moore, V. C.; O'Connel, M. J.; Haroz, E. H.; Hubbard, J.; Miller, M.; Rrialon, K.; Kittrell, C.; Ramesh, S.; Hauge, R. H.; Smalley, R. E. *J. Phys. Chem. B* **2003**, *107*, 6979−6985.

(32) Saito, R.; Jorio, A.; Hafner, J. H.; Lieber, C. M.; Hunter, M.; McClure, T.; Dresselhaus, G.; Dresselhaus, M. S. *Phys. Rev. B* **2001**, *64*, 085312.

(33) Okazaki, K.; Nakato, Y.; Murakoshi, K. *Phys. Rev. B* **2003**, *68*, 035434.

(34) Ericson, L. M.; Pehrsson, P. E. *J. Phys. Chem. B* **2005**, *109*, 20276−20280.

(35) Song, C.; Pehrsson, P. E.; Zhao, W. *J. Mater. Res.* **2006**, *21*, 2817−2823.

(36) Awichi, A.; Tee, E. M.; Srikanthan, G.; Zhao, W. *Appl. Spectrosc.* **2002**, *56*, 897−901.

(37) Badugu, R.; Lakowicz, J. R.; Geddes, C. D. *Anal. Chem*. **2004**, *76*, 610−618.